scientific data

Check for updates

OPEN

DATA DESCRIPTOR

Concurrent single-pulse TMS-fMRI dataset to reveal the causal connectome in healthy and patient populations

Cameron Glick[1,4], Niharika Gajawelli[1,4], Yinming Sun[2], Faizan Badami[3], Manish Saggar[1,5] ✉ & Amit Etkin[3,5]

Neuroimaging and cognitive neuroscience studies have identified neural circuits linked to anxiety, mood, and trauma-related symptoms and focused on their interaction with the medial prefrontal default mode circuitry. Despite these advances, developing new neuromodulatory treatments based on neurocircuitry remains challenging. It remains unclear which nodes within and controlling these circuits are affected and how their impairment is connected to psychiatric symptoms. Concurrent single-pulse (sp) TMS/fMRI offers a promising approach to probing and mapping the integrity of these circuits. In this study, we present concurrent spTMS/fMRI data along with structural MRI scans from 152 participants, across 4 clinical groupings: Non-trauma Exposed Healthy Controls (NTHC; n = 46), Trauma Exposed Healthy Controls (TEHC; n = 29), Non-trauma Induced Symptomatic (NTS; n = 43), Trauma Induced Symptomatic (NIS; n = 34).The spTMS was administered to 11 different cortical sites, providing a dataset that allows researchers to investigate how brain circuits are modulated by spTMS.

Background & Summary

Information flow in the resting human brain can be organized into functional networks[1,2] which can be characterized as the pathways by which information passes between brain regions[3]. The dynamics underpinning these functional networks has been the subject of a vast body of research[4,5], but how these networks directly impact or instigate information flow has not yet been elucidated. Specifically, there is a lack of causal evidence for how the propagation of information across the brain occurs. In order to address this fundamental question; how region-region information flow is mediated by these networks, we integrate transcranial magnetic stimulation (TMS) and functional magnetic resonance imaging (fMRI). TMS generates a short magnetic pulse which induces an electric field in a targeted brain region. TMS has been shown, not only to influence local activity at the target site, but also in distal regions[6,7]. This suggests that observed modulation of activity in distally-connected brain regions could be the result of activity propagation through intrinsic connectivity to the stimulation site.

Single TMS pulses can probe the integrity of these circuits, while repetitive TMS (rTMS) can modulate cortical activity—high-frequency rTMS enhances activity, while low-frequency rTMS suppresses it. The primary goal of a single rTMS session is to determine if it can temporarily improve brain abnormalities in patients and be used as a target for future interventions rather than to create lasting therapeutic changes.

By integrating TMS with concurrent fMRI (TMS/fMRI), we can visualize how localized TMS affects widespread downstream neural circuits. This combined approach offers insights into how different prefrontal TMS nodes regulate these circuits and whether such effects differ in patients with anxiety, depression, or trauma-related symptoms—populations that have been unexplored in concurrent TMS/fMRI studies.

We provide a comprehensive TMS/fMRI dataset that includes resting-state recordings and single-pulse TMS-fMRI data[8]. This dataset enables the exploration of cortical activity changes induced by spTMS at 11 different sites in both trauma-exposed and non-trauma-exposed healthy participants, as well as in trauma-induced

[1]Department of Psychiatry and Behavioral Sciences, Stanford University, Stanford, CA, USA. [2]Department of Psychiatry, University of California San Diego, San Diego, CA, USA. [3]Alto Neuroscience, Los Altos, CA, USA. [4]These authors contributed equally: Cameron Glick, Niharika Gajawelli. [5]These authors jointly supervised this work: Manish Saggar, Amit Etkin. ✉e-mail: saggar@stanford.edu

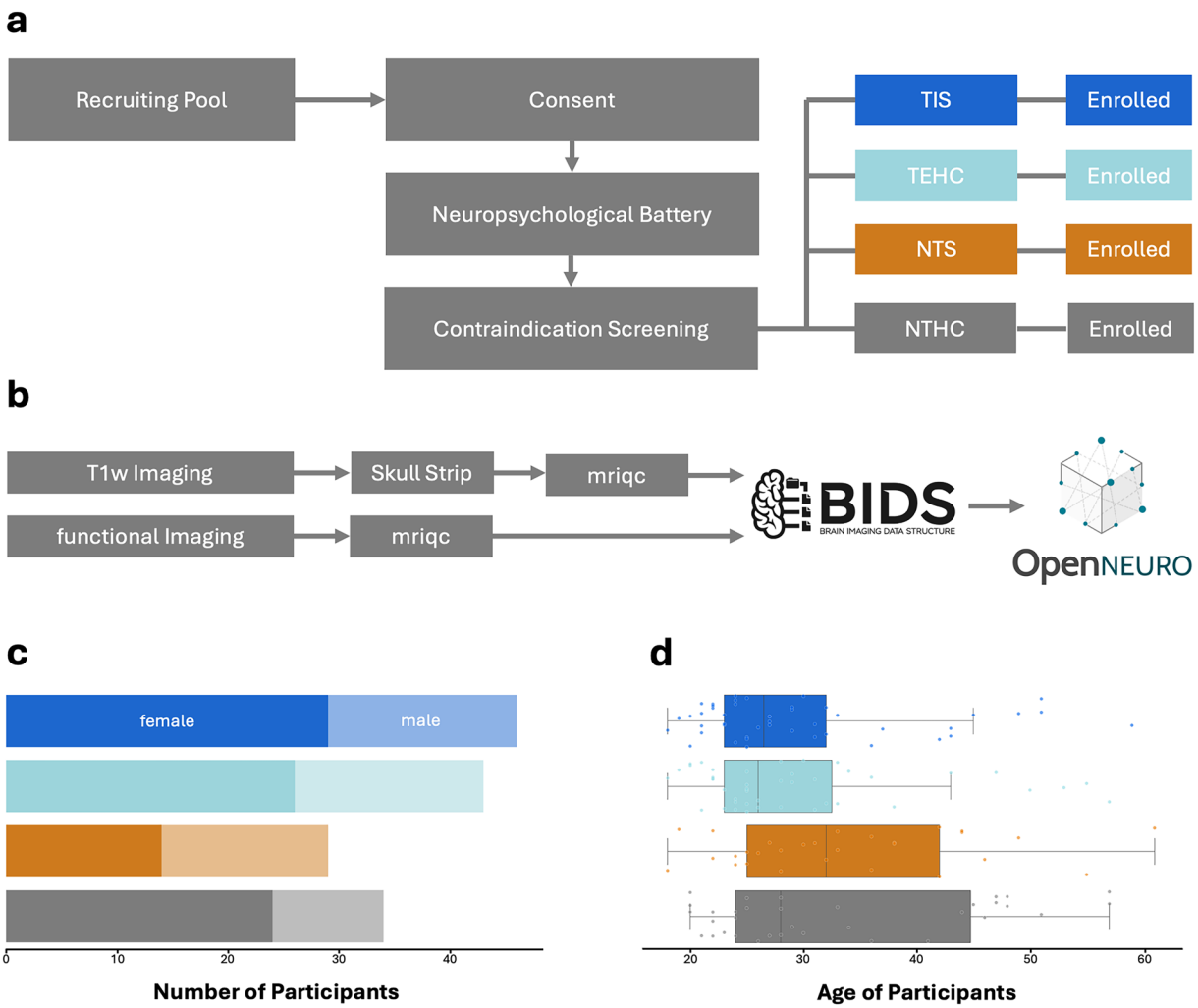

Fig. 1 (**a**) Recruitment Pipeline. Every participant undergoes a screening process and is then separated into one of 4 groups. (**b**) Imaging pipline. (**c**) Gender balance per group for all reported participants. (**d**) Age per group for all reported participants.

and non-trauma symptomatic depressed participants. The resting-state data can be used to assess changes in functional connectivity metrics, while the spTMS data allows for investigating spatiotemporal brain changes across different stimulation sites.

The dataset provides a unique opportunity to investigate the relationship between trauma-related circuit disruptions, deficits in core functions such as emotion regulation and executive function, and patient-specific TMS/fMRI mapping. By enabling the study of personalized targeting of prefrontal pathways, the dataset contributes to a deeper understanding of brain circuitry in trauma and related conditions. This data is completely novel and has not yet been used.

Methods

Participant population. Participants were recruited via advertisements requesting participants who were interested in "a study identifying causal connectome mechanisms of the human brain". Each participant was asked to participate in 2–5 study visits, the first of which included consent, intake, and neuropsychological test; the second: anatomical T1 and fMRI data acquisition; the third: TMS/fMRI scans; the fourth and fifth: miscellaneous data collection if previously missed. This release reports a majority subset of the data collected from the second, third, and sometimes fourth study visits. Due to constraints on scan time, intolerability of specific stimulation sites for some participants, unusable noisy data, and the addition of some targets after the start of the study, not all participants completed all TMS/fMRI runs.

Participants were asked to provide consent for 2–5 days of data collection spread over 4 weeks. Participants consented to have their data maintained, anonymized, and distributed for future research. All participation in the study was monitored by trained study staff. The study was approved and monitored by the Stanford University Institutional Review Board: 31244. Participants were excluded if they demonstrated or reported any significant neurological pathology, e.g., loss of consciousness >30 mins, post-trauma amnesia >24 hrs. Furthermore, exclusion criteria included claustrophobia and the use of psychiatric medication. Doctoral-level clinicians administered the *Structured Clinical*

Shorthand Name	X (MNI)	Y (MNI)	Z (MNI)	Schaefer Parcel	Schaefer Network	Site Discovery	Number of NTHC Scans	Number of TEHC Scans	Number of NTS Scans	Number of TIS Scans
R-FP	24	60	−2	83	Control Network	EEG	33	24	34	29
L-FP	−24	60	−2	45	Default Mode Network	EEG	27	23	33	29
R-FEF	34	6	62	86	Control Network	Previous Work	41	23	39	34
R-IFJ	50	10	28	72	Dorsal Attention	Previous Work	39	27	39	29
R-IPL	48	−54	46	82	Control Network	Previous Work	29	23	27	27
R-M1	40	−18	64	64	Somatomotor Network	Anatomical Imaging	41	23	39	32
R-preSMA	6	2	70	78	Salience Network	Previous Work	36	20	36	28
R-aMFG	30	50	26	85	Control Network	ICA	41	24	37	33
L-aMFG	−32	42	34	27	Salience Network	ICA	40	24	37	31
R-pMFG	46	26	38	86	Control Network	ICA	43	23	37	32
L-pMFG	−38	22	48	47	Default Mode Network	ICA	42	23	38	32
Resting	N/A	N/A	N/A	N/A	N/A	N/A	46	29	43	30

Table 1. Summary of all scan files and stimulated sites included in the data release.

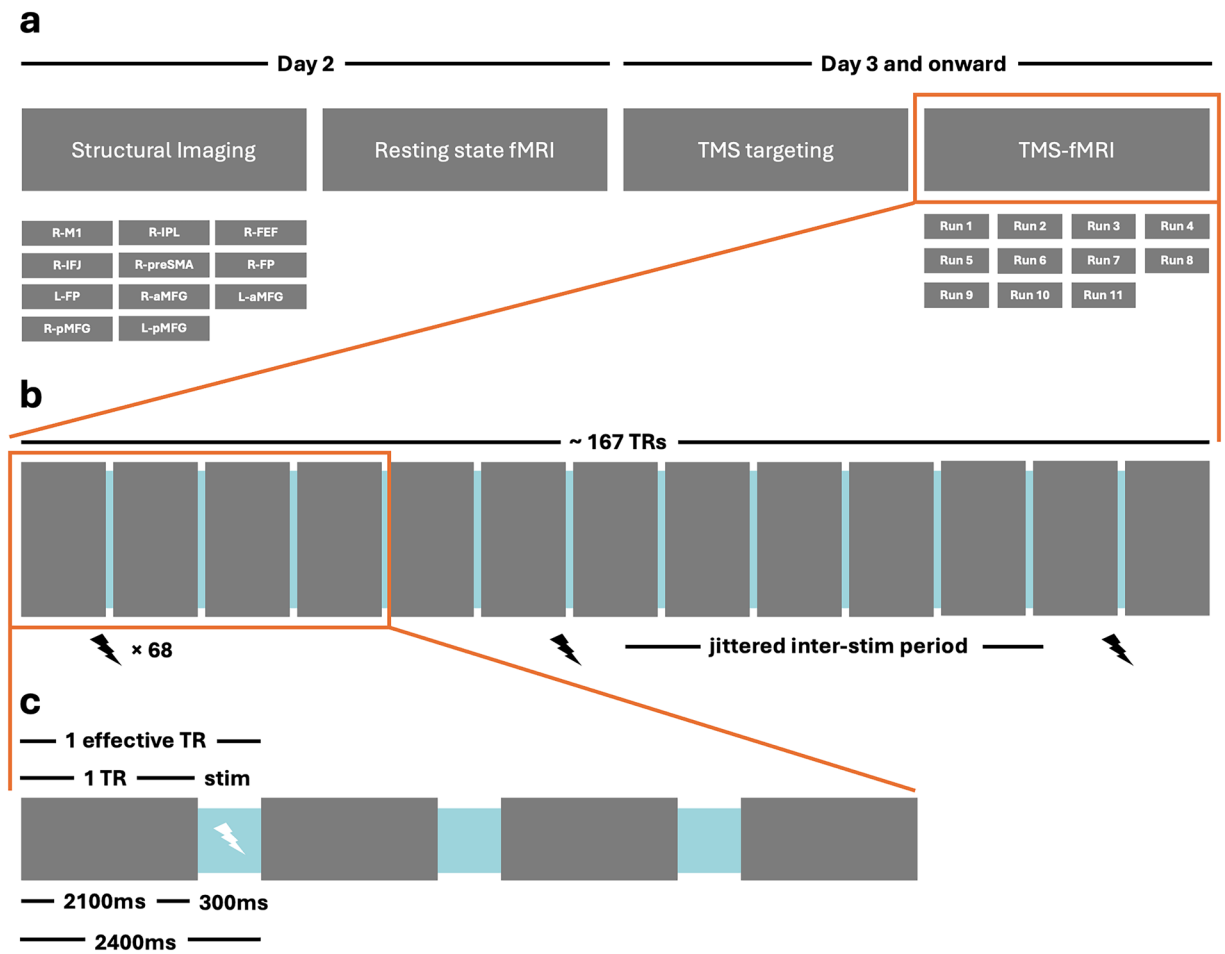

Fig. 2 Project Timeline and Stimulation Paradigm at different resolutions. (**a**) Study consists of 2 sessions, the first being MRI acquisition without TMS, and the second including TMS. There were 11 TMS-fMRI runs, each corresponding to an identified cortical region from day 1. (**b**) The concurrent TMS-fMRI period lasts for ~167 effective TRs where an effective TR is 2400 ms. (**c**) 1 Effective TR = 2400 ms where 1 Actual TR = 2100 ms. A 300 ms gap is left in which stimulation may or may not occur. Stimulation occurs on a jittered 6-7 TR basis.

Interview for DSM-IV Disorders to characterize current and past psychiatric pathologies in participants. Participants were then grouped into 4 cohorts, each representing a subsample of the study population. The cohorts are as follows: Non-Trauma Healthy Control (NTHC), Trauma Exposed Healthy Control (TEHC), Non-Trauma Symptomatic (NTS), and Trauma-Induced Symptomatic (TIS) (Fig. 1a). Throughout the study, participants were encouraged to report any physical or psychological discomfort and could withdraw at any time.

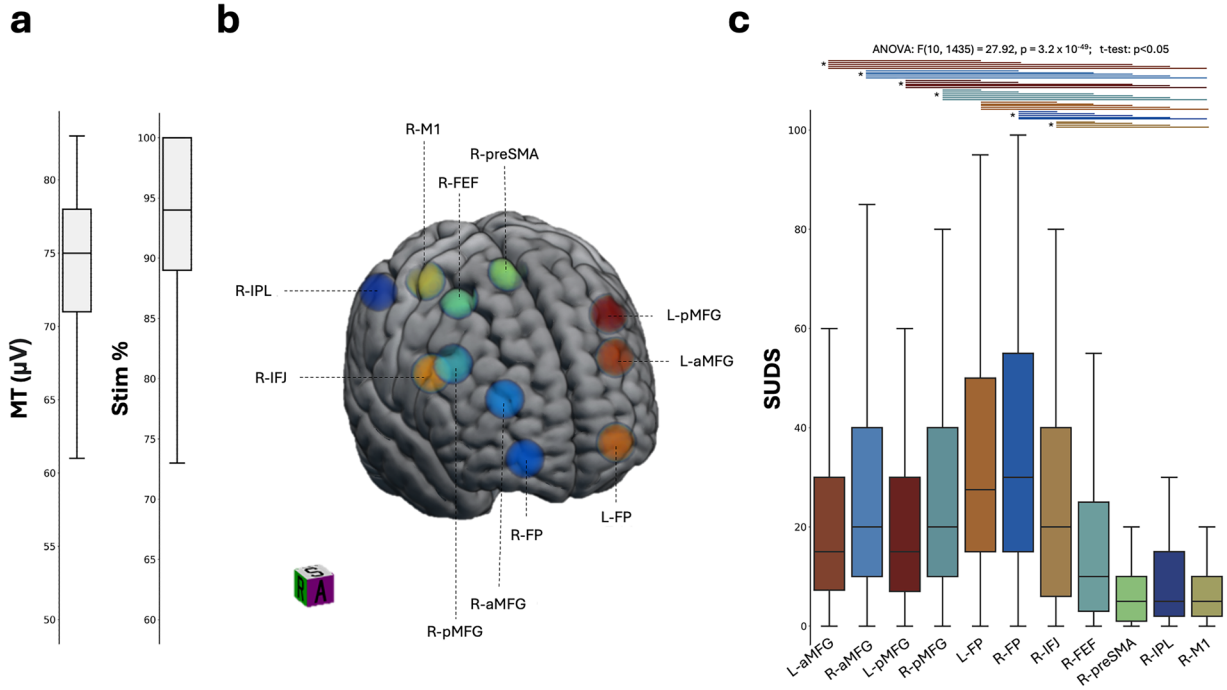

Fig. 3 Summary of stimulation data. (**a**) Motor Threshold and Stimulation Percentage across all participants. (**b**) Stimulation sites. (**c**) Subjective Units of Distress Scale across all participants grouped by stimulation site.

Participant assessment and clinical grouping. Prior to neuroimaging data acquisition, participants underwent a comprehensive evaluation consisting of structured interviews, neuropsychological assessments, and self-report questionnaires. These measures were used to determine a participant's clinical grouping.

The initial questionnaire collected demographic information, including but not limited to age, sex assigned at birth, ethnicity, and race. Subsequent, validated self-report instruments, included the Generalized Anxiety Disorder-7 (GAD-7) for anxiety screening, the Patient Health Questionnaire-9 (PHQ-9) for depression screening, the Posttraumatic Stress Disorder Checklist for DSM-5 (PCL-5) for PTSD screening, and the Fear, Anxiety, and Stress (FAS) scale to evaluate related psychological constructs.

A trained clinician then conducted a structured clinical interview to establish participants' medical history and current mental health status. The same clinician administered the Wechsler Abbreviated Scale of Intelligence (WASI-II) to assess intellectual functioning and the Clinician-Administered PTSD Scale for DSM-5 (CAPS-5) to evaluate PTSD symptomatology in accordance with DSM-5 criteria. Summary statistics for these measures, along with additional metrics, are presented in Table 3.

Anatomical imaging. All structural scanning was performed at the Stanford School of Medicine Richard M. Lucas Center for Imaging. Images were captured on 3 Tesla GE MR750 scanners with 8-channel head coils. T1 weighted (3D inversion SPGR) images were collected to serve as TMS targeting data for the following sessions. Optimized scan parameters were as follows: acquisition resolution = 1.0 × 0.9 × 0.9 mm, Flip Angle = 15 deg, FOV = 22 cm, Inversion Time = 450 ms, matrix = 256 × 256, Slices = 184, TE = 3.4 ms, TR = 8.6 ms.

fMRI Data collection. We report an 8-minute resting state functional Magnetic Resonance Imaging (rs-fMRI) run performed in the same GE MR750 setup. T2-weighted gradient echo spiral in/out pulse sequence (SPRLIO) whole-brain scans with 29 4 mm axial slices, Excitations = 2, Flip Angle = 80 deg, FOV = 22 cm, matrix = 64 × 64, Pixel Size = 3.4 mm, Slice Spacing = 0.8 mm, TE = 30 ms, TR = 2000ms, Volumes = 240 were collected from every participant.

TMS sites-targeting. We report 11 TMS/fMRI runs, one for each cortical target (Table 1). Each run consisted of 68 jittered single-pulse TMS doses targeted to a cortical site from the following list: left/right anterior middle frontal gyrus (L/R-aMFG), left/right frontal pole (L/R-FP), left/right posterior middle frontal gyrus (L/R-pMFG), right frontal eye field (R-FEF), right inferior frontal joint (R-IFJ), right inferior parietal lobe (R-IPL), right primary motor area (R-M1), and right pre-supplementary motor area (R-preSMA) (Table 1, Fig. 3b). The choice of stimulation site locations (MNI coordinates) depended on previous literature[9]).

Prior to TMS/fMRI acquisition, T1 weighted images were used to identify the loci of TMS targets for each participant in the MNI space. These were then co-registered with the head position using the Visor[2] software and projected to the individual's native space. The loci of targeted cortical stimulation were annotated on a Lycra swim cap worn by the individual in the scanner.

Region 1	Region 2	P-value
L-aMFG	L-FP	0.0001
L-aMFG	R-FP	<0.0001
L-aMFG	R-preSMA	<0.0001
L-aMFG	R-IPL	0.0002
L-aMFG	R-M1	<0.0001
R-aMFG	R-FP	0.003
R-aMFG	R-FEF	0.0003
R-aMFG	R-preSMA	<0.0001
R-aMFG	R-IPL	<0.0001
R-aMFG	R-M1	<0.0001
L-pMFG	L-FP	0.0001
L-pMFG	R-FP	<0.0001
L-pMFG	R-preSMA	<0.0001
L-pMFG	R-IPL	0.0003
L-pMFG	R-M1	0.0001
R-pMFG	L-FP	0.0144
R-pMFG	R-FP	0.0002
R-pMFG	R-FEF	0.0049
R-pMFG	R-preSMA	<0.0000
R-pMFG	R-IPL	<0.0000
R-pMFG	R-M1	<0.0000
L-FP	R-IFJ	0.0022
L-FP	R-FEF	<0.0001
L-FP	R-preSMA	<0.0001
L-FP	R-IPL	<0.0001
L-FP	R-M1	<0.0001
R-IFJ	R-FEF	0.0461
R-IFJ	R-preSMA	<0.0001
R-IFJ	R-IPL	<0.0001
R-IFJ	R-M1	<0.0001
R-FP	R-IFJ	0.0461
R-FP	R-FEF	<0.0000
R-FP	R-preSMA	<0.0000
R-FP	R-IPL	<0.0000
R-FP	R-M1	<0.0000

Table 2. Summary of significant pairwise comparisons between reported SUDS grouped by region.

Concurrent TMS/fMRI data collection. A figure-eight, MRI-compatible, TMS coil (MagPro MRi-B91) was set up to deliver biphasic magnetic stimulations. This apparatus was fixed inside the scanner bore via a custom mount and connected to a MagPro X100 stimulator via a patch panel with a powerline filter. Field inhomogeneity resulting from the TMS apparatus was addressed by implementing an automated higher-order shimming optimized for SPRLIO prior to each run. Concurrent TMS/fMRI necessitated using a TMS-compatible single-channel head coil optimized to minimize spatial concerns. MRI parameters mirror those listed in rs-fMRI except for a few key differences. A modified Flip Angle = 85 deg, Spacing = 1 mm, Volumes = 167 were used. Additionally, an extended TR = 2400 ms generated a temporal gap in which single TMS pulses can be interleaved. The TR was set to be 2100 ms with a 300 ms break, creating an effective TR = 2400 ms. Leveraging this break, TMS could be applied without affecting MRI acquisition (Fig. 2b,c). Prior to the participant entering the scanner, the Motor Threshold was established using the same TMS apparatus used for concurrent TMS/fMRI collection. Motor threshold and location of maximal stimulation were determined by applying single pulses to the right motor cortex and observing hand twitch responses. MT was defined as the level at which 5/10 consecutive trials resulted in a noticeable motor response in the participant's hand after pulses to the location of maximal stimulation. All TMS pulses during the TMS/fMRI paradigm were administered at 120% of the established motor threshold (Fig. 3a).

Each TMS/fMRI run consisted of single pulses with jittered interstimulus intervals ranging from 1 to 6 TR. In total, 68 stimulations were delivered over 6 min 41 secs (max of 167 effective TRs). The TMS apparatus and coil were reset and repositioned for every stimulation site. This procedure was conducted while the participant was still on the table but while the table was extended away from the bore. The order by which each stimulation site was set up and then assessed was randomized to address any confounding order that may be present in the data. Participants were provided with ear protection to minimize the impact of the combined TMS and MRI noise. Additionally, participants wore a GE pulse oximeter and a mid-thoracic strain gauge sampled at 50 Hz to measure heart rate and respiration, respectively. Participants were prompted to provide their level of discomfort following every run by asking: "Please

For Each participant the following variables are provided	
Clinical Grouping	NTHC, TEHC, NTS, TIS = No Trauma Healthy Control, Trauma Exposed Healthy Control, No Trauma Symptomatic, Trauma Induced Symptomatic
ID	1000 s, 2000s, 3000 s, 4000 s corresponding to the above clinical groupings. e.g. NTHC1001, TEHC2001, etc.
Age	Age in years
Sex assigned at birth	1 = F, 2 = M
Ethnicity	1 = American Indian or Alaska Native, 2 = Asian, 3 = Black or African American, 4 = Native Hawaiian or Other Pacific Islander, 5 = White, 6 = Multiple Races, 7 = Other, 8 = N/A
Race	1 = Non-Hispanic, 2 = Hispanic, 3 = N/A
Years of Education	Duration in years
PHQ-9 Score	Patient Health Questionnaire 9 Raw Score
GAD-7 Score	General Anxiety Disorder 7 Raw Score
CAPS-5 Score	Clinician-Administered PTSD Scale for DSM-5 Raw Score of Past Month and Lifetime
PCL-5 Score	Posttraumatic Stress Disorder Checklist for DSM-5 Raw Score
WASI-II Score	Wechsler Abbreviated Scale of Intelligence II Raw and T-scores
FAS Score	Fear, Anxiety, and Stress Score Raw and Percentile
Motor Threshold	Value in microvolts
Stimulation Percent	Value in percent
SUDS	Subjective Units of Distress/Discomfort range 0–100
BOLD Signal	BIDS formatted scans
Criterion_Trauma	Participant Meets Trauma Criterion A Boolean 0,1 value
Current <Disorder> Diagnosis	Current Diagnosis of Disorder Boolean 0,1 value
Lifetime <Disorder> Diagnosis	Lifetime Diagnosis of Disorder Boolean 0,1 value
<Type> Phobia	Participant Has Phobia Boolean 0,1 value
<Substance> Use	Participant Uses Substance Boolean 0,1 value
Urine Tox Results	Drug Urine Screen Positive Result Boolean 0,1 value
Diagnosis Other Misc	Non-listed Diagnosis Boolean 0,1 value
No Diagnosis	Boolean 0,1 value

Table 3. Summary of all variables included in the data release.

rate your pain or discomfort from 1 to 100, '0' meaning 'no pain' and '100' meaning 'the worst pain you can imagine." (The Subjective Units of Distress (SUDS) scale) (Fig. 3b-c, Table 2) Furthermore, participants were notified they could discontinue the experiment at any time. Stimulation to the R-FP was reported as being the most uncomfortable site. ANOVA: $F(10, 1435) = 27.92$, $p = 3.2 \times 10^{-49}$ and t-tests: $p < 0.05$ demonstrate the differences in mean reported SUDS between the stimulation sites (Table 2; Fig. 3c).

Data technical validation: assessing image quality. All collected data[8] were subdivided using two criteria: Group, e.g., NTHC or TIS, and whether the data was collected during resting state or stimulation. For the stimulation data, the TR was changed to 2400 ms post-acquisition to incorporate the 300 ms break between the TMS pulses. This was done using the *fslmerge* function from FSL[10–12] Data was then partially preprocessed via the *mriqc* software package, which provided a host of Image Quality Metrics (IQMs) to describe the data[13]. A subset of IQMs was then selected and reported for data grouped by fMRI paradigm and data grouped by group.

To assess the quality of the MR scans across clinically grouped individuals, participants were broken into 4 categories: NTHC, NTS, TEHC, and TIS. The tSNR, SNR, and mean FD were computed for each group and compared between stimulation and resting state. This demonstrates the similarities and differences between groups and fMRI data acquisition paradigms. Post-hoc t-tests demonstrate that SNR and Mean FD vary between clinical groupings during periods of stimulation ($p < 0.01$) (Fig. 4b).

For data grouped by fMRI paradigm (resting or TMS), we report Spatial Metrics: Entropy-focus criterion[14], Foreground-Background energy ratio[15], Signal-to-Noise Ratio (SNR); Temporal Metrics: DVARS[16] (D referring to the temporal derivative of time courses, VARS referring to RMS variance over voxels), Global Correlation[17] (GCOR), TSNR[18] (Temporal SNR); and Artifact Metrics: Framewise Displacement[19] (FD)), Ghost to Signal Ratio[20] (GSR), AFNI's outlier ratio (AOR), and AFNI's quality index (AQI). These IQMs were compared to the open source mriqc dataset[21]. The mriqc database was scrubbed of outliers 5 times the interquartile distance away from the mean for easy plotting and comparison to the collected dataset. The collected data was not modified. While the data quality between the aforementioned data and established fMRI data remain quite similar, p-values derived from post-hoc t-tests demonstrate the differences in each measure. EFC, FBER, SNR, DVARS, TSNR, and Mean FD from the collected data outperform metrics from the fmriqc dataset (Fig. 4c).

Data sharing. The aforementioned de-identified data[8] were posted and will be periodically updated on the OpenNeuro website[22]. All subject data has been anonymized and defaced. Furthermore, all identifiable information (HIPAA 18 factors) have been removed from our long term storage. The data are organized via the Brain Imaging Data Structure[23] (BIDS version (v1.9.0 guidelines). As the BIDS guidelines dictate, data has been

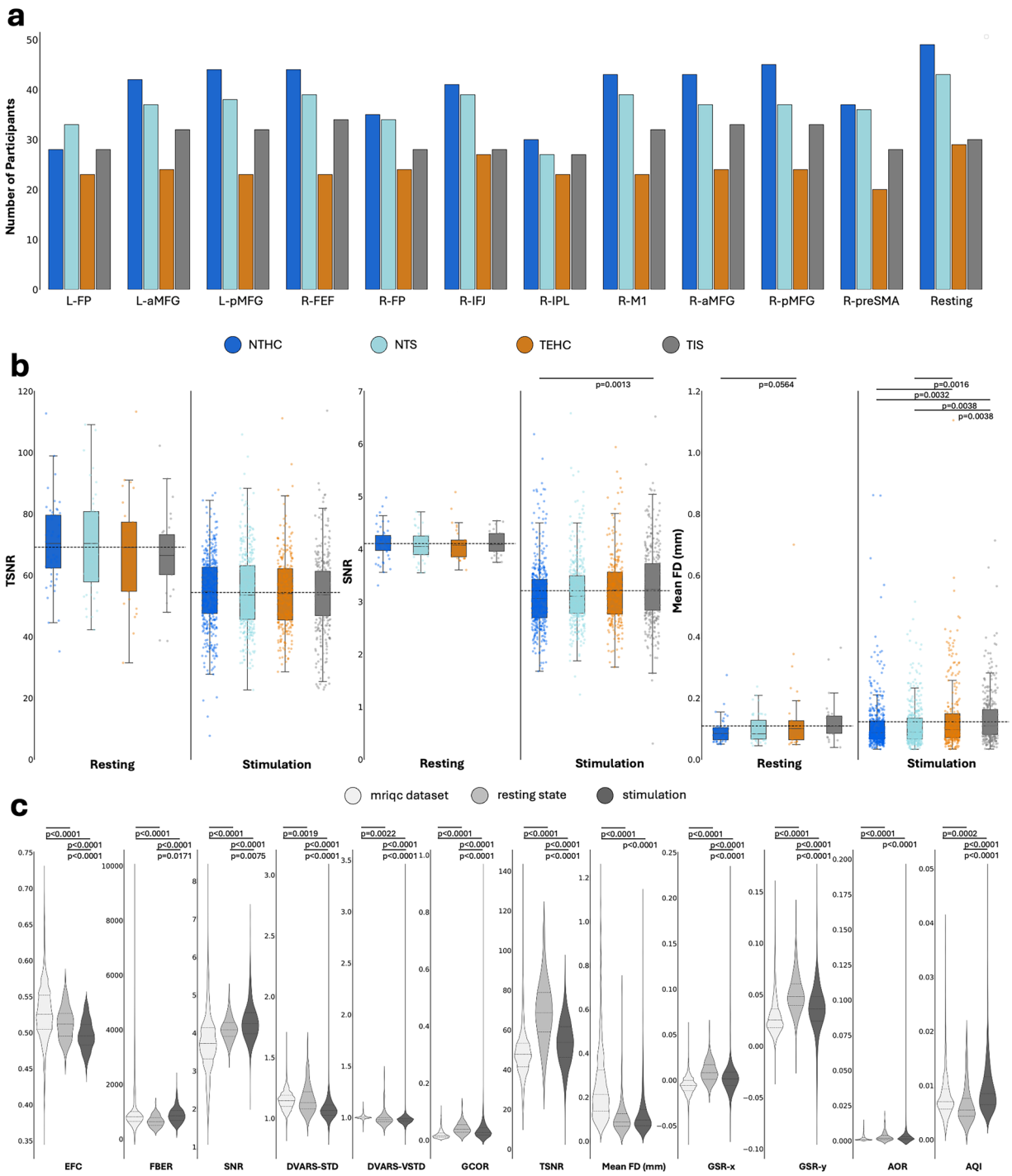

Fig. 4 Image Quality Metrics. (**a**) Quantity of data broken down by imaging/stimulation target. (**b**) A comparison of TSNR, SNR, and Mean FD across clinical groupings. The Dashed line represents the mean across groups. (**c**) A comparison of group level Image Quality Metrics as compared to the mriqc database deplete of outliers greater than 5 IRQs from mean.

organized into nested files with standardized names. Acquired data are converted to NIFTI format with associated metadata stored in JSON files. Subjects are organized into four categories: NTHC, NTS, TEHC, and TIS (Fig. 1a,b).

Data Records

All imaging data associated with the study are posted at Open Neuro under the name (OpenNeuro Dataset ds005498, https://openneuro.org/datasets/ds005498). The dataset[8] comprises 152 subjects categorized into four groups: NTHC, TEHC, NTS, and TES, with IDs in the 1000 s, 2000 s, 3000 s, and 4000 s, respectively (Fig. 1c). All data has been de-identified. The labeling of the data is as follows:

Structural data: sub-XXXX_ses-Y_run-Z_T1w.ext,

Summary Table of Participant Population					
Primary Characteristic	**Secondary Characteristic**	**NTHC**	**TEHC**	**NTS**	**TIS**
Number of Participants		46	29	43	34
Age (Years), (SD)		30 (10)	34 (11)	30 (10)	33 (12)
Sex assigned at birth, n (%)	Male	36.96	51.72	39.53	26.47
	Female	63.04	48.28	60.47	70.59
Ethnicity, n (%)	Hispanic	23.91	13.79	11.63	20.59
	Non-Hispanic	73.91	86.21	74.42	79.41
	N/A	2.17	0.00	13.95	0.00
Race, n (%)	American Indian or Alaska Native	0.00	0.00	0.00	0.00
	Asian	30.43	31.03	18.60	11.76
	Black or African American	2.17	0.00	4.65	2.94
	Native Hawaiian or Other Pacific Islander	4.35	6.90	0.00	2.94
	White	45.65	51.72	53.49	58.88
	Multiple Races	6.52	3.45	13.95	8.82
	Other	8.70	6.90	9.30	14.71
	N/A	2.17	0.00	0.00	2.94
Years of Education (Years), (SD)		16 (2)	16 (2)	16 (2)	15 (2)
PHQ-9 Score (Average), (SD)		1 (2)	1 (1)	16 (4)	16 (3)
GAD-7 Score (Average), (SD)		1 (1)	1 (1)	12 (5)	15 (5)
CAPS Score (Average), (SD)	Last Month	2 (4)	3 (4)	29 (25)	52 (22)
	Lifetime	9 (13)	11 (11)	55 (31)	85 (21)
PCL Score (Average), (SD)		19 (7)	19 (3)	50 (16)	59 (13)
WASI Score (Average), (SD)	Vocabulary T Score	58 (7)	59 (9)	58 (11)	57 (8)
	Matrix T Score	60 (6)	58 (7)	60 (9)	59 (6)
	Matrix Total Score	118 (10)	117 (13)	117 (16)	116 (12)
FAS Score (Average), (SD)	Score	43 (12)	44 (9)	41 (10)	42 (20)
	Percentile	44 (27)	48 (24)	39 (25)	38 (31)

Table 4. Summary of demographics reported by each clinical grouping.

Functional data: sub-XXXX_ses-Y_task-TYPE_MNI_COORDINATES.ext,

where XXXX is the subject ID, Y is the session number, Z indicates the run number, TYPE refers to the type of fMRI scan (either resting or stimulation), and *ext* represents the file extension (.nii, .nii.gz, or .json).

For stimulation tasks, the naming convention also specifies the MNI coordinates out of the 11 available, and the associated brain network. For example, "stim24 × 60 × Minus2" denotes stimulation at X = 24, Y = 60, Z = −2 locations of the MNI coordinates. A glossary of variables contained in the data release can be found in Table 3 and the availability of scans per group is quantified in Table 1. (Tables 1, 3).

Technical Validation

To assess the quality of the collected data, we took a three-step approach. First, we assessed the quantity. Second, we hierarchically grouped the data to tease out differences between clinical groups and between resting state fMRI and TMS-fMRI. Finally, we compared the collected data with the *mriqc* public dataset.

Participants and data quantity. 333 healthy participants (204 F, 127 M, 2 unreported) were recruited with a mean age of 32 years (SD: 11). Of these 333 recruited participants, we report data from 152 individuals (93 F, 52 M, Mean age 31.1 yr, SD age 10.5 yr) (Fig. 1c, Table 4). The quantity of present data differs between groups (Fig. 1c). When examining the number of reported participants assigned to individual groups, NTHC reports the largest number of participants at 46, and TIS reports the lowest number of participants at 34. On average, NTHC group consistently reports the most data across both resting-state and TMS/fMRI, with a total completion rate of 78.6% across all individuals. TEHC group reports the lowest total completion at 47.8% across all individuals. Differences in data completion are attributed to participant dropouts and/or incompletion of all 11 TMS targets (Fig. 4a).

Functional data quality. When compared between groups, the reported IQMs (TSNR, SNR, Mean FD) remain consistent (Fig. 4b). This demonstrates the robustness of the scan protocol to varying healthy and clinical populations. Furthermore, the lack of variance in average IQMs across clinical groups allows future valid comparisons between sub-groups. Resting-state fMRI average TSNR and SNR outperformed TMS/fMRI IQMs at the clinical subgroup and group levels. This is to be expected as introducing TMS apparatus into the scanner bore impacts scan quality. Notably, the mean FD during stimulation was slightly higher than the mean FD during rest. This could be due to the added stress of the TMS apparatus or the added pressure on participants to remain still during stimulation. Despite the reduction in scan quality during TMS/fMRI, all reported IQMs for all clinical groups and scanning paradigms stay within the acceptable ranges.

Functional data compared to canonical data. To assess the quality of our collected fMRI data, we first split the data into two subgroups: rfMRI and TMS/fMRI. These two groups were then compared to the *mriqc* published dataset via key IQMs (Fig. 4c). Our collected data remained similar to the published dataset, so we believe the data maintains a quality consistent with previously published fMRI datasets.

Usage Notes

The data were organized using the BIDS naming convention, employing key-value pairs such as "sub-value," "run-value," and "task-value." The "sub" key represents study participants. The "run" key denotes separate T1-weighted (T1w) data acquisitions for the same subject during the same session using consistent parameters. The "task" key is used for BOLD (Blood Oxygenated Level Dependent) fMRI data and identifies either resting-state activity or one of the 11 stimulation sites detailed in the methods section.

Most participants had their structural and resting-state data collected in one session, with stimulation data gathered in a separate session. However, some participants underwent more than two sessions for data collection. In cases where structural and resting-state data were not collected during the first session, these participants may have their data recorded in subsequent sessions, and session one may be absent for them.

To ensure anonymization, the structural data was defaced using PyDeface (https://pypi.org/project/pydeface/), as recommended by OpenNeuro.

Code availability

Additional data and all processing and QC code are posted to the Brain Dynamics Lab GitHub https://github.com/braindynamicslab/sptmsfmri.

Received: 14 November 2024; Accepted: 10 June 2025;
Published online: 01 July 2025

References

1. Power, J. D. *et al.* Functional network organization of the human brain. *Neuron* **72**, 665, https://doi.org/10.1016/j.neuron.2011.09.006 (2011).
2. Deco, G., Jirsa, V. K. & McIntosh, A. R. Emerging concepts for the dynamical organization of resting-state activity in the brain. *Nature Reviews Neuroscience 2011* **12**:1 12, 43–56. https://doi.org/10.1038/nrn2961 (2010).
3. Cole, M. W., Ito, T., Bassett, D. S. & Schultz, D. H. Activity flow over resting-state networks shapes cognitive task activations. *Nat. Neurosci.* **19**, 1718–1726, https://doi.org/10.1038/nn.4406 (2016).
4. Mišic, B. *et al.* Network-Level Structure-Function Relationships in Human Neocortex. *Cereb. Cortex* **26**, 3285–3296, https://doi.org/10.1093/cercor/bhw089 (2016).
5. Gollo, L. L., Roberts, J. A. & Cocchi, L. Mapping how local perturbations influence systems-level brain dynamics. *Neuroimage* **160**, 97–112, https://doi.org/10.1016/j.neuroimage.2017.01.057 (2017).
6. Bestmann, S. *et al.* Mapping causal interregional influences with concurrent TMS–fMRI. *Exp. Brain Res.* **191**, 383–402, https://doi.org/10.1007/s00221-008-1601-8 (2008).
7. Ruff, C. C., Driver, J. & Bestmann, S. Combining TMS and fMRI: From 'virtual lesions' to functional-network accounts of cognition. *Cortex* **45**, 1043–1049, https://doi.org/10.1016/j.cortex.2008.10.012 (2009).
8. Glick, C. *et al. OpenNeuro Dataset ds005498 (Single-pulse TMS fMRI), [Dataset]* https://doi.org/10.18112/openneuro.ds005498.v1.1.0 (2024).
9. Toll, R. T. *et al.* An electroencephalography connectomic profile of posttraumatic stress disorder. *Am. J. Psychiatry* **177**, 233–243, https://doi.org/10.1176/appi.ajp.2019.18080911 (2020).
10. Woolrich, M. W. *et al.* Bayesian analysis of neuroimaging data in FSL. *Neuroimage* **45**, S173–86, https://doi.org/10.1016/j.neuroimage.2008.10.055 (2009).
11. Smith, S. M. *et al.* Advances in functional and structural MR image analysis and implementation as FSL. *Neuroimage* **23**(Suppl 1), S208–19, https://doi.org/10.1016/j.neuroimage.2004.07.051 (2004).
12. Jenkinson, M., Beckmann, C. F., Behrens, T. E. J., Woolrich, M. W. & Smith, S. M. FSL. *Neuroimage* **62**, 782–790, https://doi.org/10.1016/j.neuroimage.2011.09.015 (2012).
13. Esteban, O. *et al.* MRIQC: Advancing the automatic prediction of image quality in MRI from unseen sites. *PLoS One* **12**, e0184661, https://doi.org/10.1371/journal.pone.0184661 (2017).
14. Atkinson, D., Hill, D. L. G., Stoyle, P. N. R., Summers, P. E. & Keevil, S. F. Automatic correction of motion artifacts in magnetic resonance images using an entropy focus criterion. *IEEE Trans. Med. Imaging* **16**, 903–910, https://doi.org/10.1109/42.650886 (1997).
15. *Frontiers*. https://www.frontiersin.org/10.3389/conf.fnins.2015.91.00047/event_abstract.
16. Power, J. D., Barnes, K. A., Snyder, A. Z., Schlaggar, B. L. & Petersen, S. E. Spurious but systematic correlations in functional connectivity MRI networks arise from subject motion. *Neuroimage* **59**, 2142, https://doi.org/10.1016/j.neuroimage.2011.10.018 (2012).
17. Saad, Z. S. *et al.* Correcting brain-wide correlation differences in resting-state FMRI. *Brain Connect.* **3**, 339–352, https://doi.org/10.1089/brain.2013.0156 (2013).
18. Krüger, G. & Glover, G. H. Physiological noise in oxygenation-sensitive magnetic resonance imaging: Physiological Noise in MRI. *Magn. Reson. Med.* **46**, 631–637, https://doi.org/10.1002/mrm.1240 (2001).
19. Jenkinson, M., Bannister, P., Brady, M. & Smith, S. Improved Optimization for the Robust and Accurate Linear Registration and Motion Correction of Brain Images. *Neuroimage* **17**, 825–841, https://doi.org/10.1016/s1053-8119(02)91132-8 (2002).
20. Giannelli, M., Diciotti, S., Tessa, C. & Mascalchi, M. Characterization of Nyquist ghost in EPI-fMRI acquisition sequences implemented on two clinical 1.5 T MR scanner systems: effect of readout bandwidth and echo spacing. *J. Appl. Clin. Med. Phys.* **11**, 170–180, https://doi.org/10.1120/jacmp.v11i4.3237 (2010).
21. Esteban, O. *et al.* Crowdsourced MRI quality metrics and expert quality annotations for training of humans and machines. *Scientific Data* **6**, 1–7 https://doi.org/10.1038/s41597-019-0035-4 (2019).
22. Markiewicz, C. J. *et al.* The openneuro resource for sharing of neuroscience data. *Elife* **10**, https://doi.org/10.7554/eLife.71774 (2021).
23. Gorgolewski, K. J. *et al.* The brain imaging data structure, a format for organizing and describing outputs of neuroimaging experiments. *Scientific Data* **3**, 1–9, https://doi.org/10.1038/sdata.2016.44 (2016).

Acknowledgements
This project was funded by an NIH R01 MH103324 awarded to A.E.

Author contributions
C.G.: data analysis, data curation, validation, writing, visualization. N.G.: data analysis, validation, data curation, writing. Y.S.: data collection, validation, and writing. F.B.: data collection, validation, and writing. M.S.: validation, writing, supervision, project administration. A.E.: conceptualization, data collection, validation, writing, supervision, funding acquisition.

Competing interests
A.E. and F.S.B. report salary and equity from Alto Neuroscience. A.E. additionally holds equity in Akili Interactive. None of the other authors has financial disclosures to report.

Additional information
Correspondence and requests for materials should be addressed to M.S.

Reprints and permissions information is available at www.nature.com/reprints.

Publisher's note Springer Nature remains neutral with regard to jurisdictional claims in published maps and institutional affiliations.